Diffusion Regularization for Iterative Reconstruction in Emission Tomography

Cyril Riddell, Habib Benali and Irène Buvat

***Abstract*— Recently, we have proposed a regularized least square criterion for adaptive regularization for reconstructing noisy SPECT data with non-uniform attenuation correction. In the present study, we show that the regularization penalty that was used is closely related to a diffusion scheme used for Gaussian filtering. For a given value of the regularization parameter, the amount of smoothing is independent from the patient attenuation map, and it is mathematically related to the full width at half maximum (FWHM) of a Gaussian filter. A second regularized least square criterion is then derived for which regularization also behaves as a diffusion scheme. The new penalty is then shown to be also applicable to the weighted least square criterion, and to the Poisson maximum likelihood criterion for PET data (i.e. without attenuation) solved by the EM algorithm. For all these criteria, the regularization strength can thus be set as the FWHM of a Gaussian filter.**

I. Introduction

Because tomographic reconstruction is an ill-posed problem, regularization is necessary to control the noise propagation from the projections into the reconstructed images. A clinically relevant approach requires knowing *a priori* the noise reduction and concomitant resolution loss due to regularization. Unfortunately, with patient dependent modeling of the data, a given regularization parameter can produce smoothing effects that differ from patient to patient. A regularization penalty previously introduced in a least square adaptive regularization technique [1] is here demonstrated to behave as a diffusion scheme for Gaussian filtering. Resolution loss is therefore set a priori as a full width at half maximum (FWHM). This regularization penalty is then extended to the weighted least square case and the OSEM algorithm for PET.

II. Theory

A. Regularized least square algorithm for SPECT

An image is estimated from a finite set of SPECT attenuated measurements by solving a linear system such as:

$$R_a f = s_a \qquad (1)$$

where f is the unknown image vector, s_a is the attenuated SPECT sinogram and R_a is a matrix that models SPECT tomographic acquisition with patient dependent non-uniform attenuation. A classical regularized least square solution of system (1) is given by minimizing:

$$\min_f \left\{ \left\| R_a f - s_a \right\|^2 + \alpha \left\| \nabla f \right\|^2 \right\} \qquad (2a)$$

where α is a scalar and ∇f is the gradient of image f. This criterion is equivalent to solving

$$(R_a^t R_a + \alpha \Delta) f = R_a^t s_a \qquad (2b)$$

where ^{t} denotes the transpose of a matrix and Δ denotes the Laplacian operator.

When modeling attenuation, matrix R_a changes with the attenuation map, whereas the Laplacian is constant. Therefore, the same regularization value α generally yields a different smoothing for different patients.

B. Diffusion regularization and approximate inversion

In a previous work [1], we have proposed to replace criterion (2) by the penalized frequency weighted least square [PFWLS] approach given by:

$$\min_f \left\{ \left\| D_S^{1/2} \left(R_a f - s_a \right) \right\|^2 + \alpha \left\| \nabla \Gamma^{-1} f \right\|^2 \right\} \qquad (3a)$$

which is equivalent to solving:

$$\left(T^t D_s T + \alpha \Delta \right) x = T^t D_s s_a \qquad (3b)$$

where $T = R_a \Gamma$, Γ represents the Chang correction, D_s stands for the ramp filtering operation in the sinogram domain, and x is such that $f = \Gamma x$. The ramp filter and Chang correction are used as a preliminary approximate inversion making the system matrix $T^t D_s T$ close to the identity matrix I, to speed convergence up and provide a normalization that allows for adaptive regularization with respect to noise [1].

In the present work, we further explore criterion (3) by considering that in system (3b), $T^t D_s T$ differs from the identity only for the effect of attenuation, and not the effect of the tomographic acquisition, and that attenuation mainly affects the low frequency content of an image. We therefore hypothesize that the regularization constraint in (3b) will produce the same filtering as the following diffusion scheme:

$$(I + \alpha \Delta) f = f_0 \qquad (4)$$

C. Riddell was with the U494 INSERM, CHU Pitié-Salpêtrière, Paris, France and GE-SMVI, Buc, France. He is now with GE Medical Systems International, Buc, France (e-mail: cyril.riddell@med.ge.com).

H. Benali and I. Buvat are with the U494 INSERM, CHU Pitié-Salpêtrière, Paris, France (e-mail: benali or buvat@imed.jussieu.fr).

0-7803-8257-9/04/$20.00 © 2004 IEEE.

where f_0 is the image to be filtered. Solution of system (4) tends towards f_0 filtered by a Gaussian kernel with FWHM equal to $3.33\sqrt{\alpha}$ [2]. We therefore say that the regularization penalty in (3) is a diffusion regularization.

An alternative approximate inversion of (1) is obtained by applying the ramp filter in the image domain [3], giving:

$$\left(D_i T^t T + \alpha\Delta\right) x = D_i T^t s_a \qquad (5)$$

where D_i stands for the ramp filtering operation in the image domain. Again, system (5) differs from the diffusion scheme (4) by the effect of attenuation only. Under the same hypothesis that attenuation mainly affects the low frequency content of an image, we expect that the Laplacian term will produce a diffusion filtering. Moreover, using the relation $\Delta x = (D_i)^2 x$, system (5) can be simplified into:

$$\left(T^t T + \alpha D_i\right) x = T^t s_a \qquad (6a)$$

which corresponds to the following penalized least square [PLS] criterion:

$$\min_f \left\{ \left\| R_a f - s_a \right\|^2 + \alpha \left\| D_i^{1/2} \Gamma^{-1} f \right\|^2 \right\} \qquad (6b)$$

where $D_i^{1/2}$ stands for the filtering of an image by the square root of the ramp filter. When based on ramp filtering, the diffusion penalty can be applied to criteria that are not derived from a prior approximate inversion of the system matrix.

C. Diffusion regularization for the weighted least square case and the OSEM algorithm

For the sake of simplicity, we describe the weighted least square criterion for the non-attenuated case only. It is expressed as:

$$\min_f \left\| \Sigma^{-1/2} \left(Rf - s \right) \right\|^2 \qquad (7)$$

where Σ is a diagonal matrix with each diagonal term equal to the weight of the corresponding measurement (e.g. its variance). Matrix R and vector s respectively replace matrix R_a and vector s_a in the non-attenuated case. The introduction of the variance of the measurements again makes the criterion dependent upon each specific patient data set. Adding a regularization constraint with fixed strength will therefore not yield uniform resolution over the reconstructed image, neither the same filtering effect from one patient to the other [4]. For constant weights Σ, diffusion regularization is obtained with the ramp filter penalty given in (6). Independence from the weights is obtained by applying a normalization diagonal operator P such as the one given in [4], which yields the following regularized criterion:

$$\min_f \left\{ \left\| \Sigma^{-1/2} \left(Rf - s \right) \right\|^2 + \alpha \left\| D_i^{1/2} \mathrm{P}^{-1} f \right\|^2 \right\} \qquad (8a)$$

equivalent to solving:

$$\left(\mathrm{P} R^t \Sigma^{-1} R \mathrm{P} + \alpha D_i \right) y = \mathrm{P} R^t \Sigma^{-1} s \qquad (8b)$$

where y is such that $f = \mathrm{P}y$.

If the variance estimates are set equal to the data mean estimates, the criterion is similar to maximizing a Poisson likelihood. This suggests that applying the same penalty based on ramp filtering to the EM algorithm should provide equivalent diffusion regularization. In this study, the penalty was implemented with the One-Step-Late method combined to the Ordered Subset acceleration technique [5], the penalty term being computed at each sub-iteration. The normalization matrix P was computed as a simple back-projection of the measurement weights.

In the case of attenuation, the Chang correction Γ should be combined to the P matrix for normalizing the weighted least square criterion [4]. With OSEM, this normalization is not straightforward any more as the algorithm already contains a normalization term for attenuation. Diffusion regularization and SPECT attenuation correction were therefore not applied to OSEM in this work.

D. Class-dependent diffusion regularization

When diffusion regularization can be applied with the Laplacian operator, it offers the additional possibility of selectively smoothing the reconstructed image by regions. Here, the regions are supposed to be defined *a priori*, for instance as classes resulting from the segmentation of the attenuation map, which keeps the problem linear. The Laplacian operator, scaled by α, can be implemented as the 4-point spatial kernel that is, at pixel k, the sum of each difference of pixel k minus its neighbors, weighted by α. A simple modification of this sum allows for a class-dependent filtering: each difference between two neighboring pixels k and l is weighted with a different "local" α, denoted α_{kl}, which determines the local level of smoothing. Since $\alpha_{kl} = \alpha_{lk}$, the system is kept symmetric. This level is held constant for all differences between pixels belonging to the same class, but can change from class to class. For a given class, it is denoted $\alpha(\text{class})$. In addition, a level of smoothing is defined between all classes that is denoted $\overline{\alpha}$. When pixels k and l belong to the same class, α_{kl} is set to $\alpha(\text{class})$, otherwise it is set to $\overline{\alpha}$. The values of $\alpha(\text{class})$ and $\overline{\alpha}$ are related to FWHM values by the same relation $3.33\sqrt{\alpha(class)}$ and $3.33\sqrt{\overline{\alpha}}$.

III. Experiments

Effectiveness of diffusion regularization was examined through simulation of attenuated SPECT data in the case of the least square criteria and non-attenuated data in the case of the OSEM algorithm.

A segmented CT slice at the heart level of the Zubal phantom [6] was considered. Activity was simulated by

setting the cardiac muscle region to 10, the blood pool region to 3, and the lung region to 2, while all other tissues were set to 1 (fig. 1, left image). This activity distribution is called "reference image" in the following.

The simulated projections of the reference image (120 projections over 360°, 128 measurement bins, parallel geometry) were of 3 types according to the attenuation map. The first type corresponded to the no attenuation case ($\mu = 0$), the second, called "Tc-99m" data, corresponded to the CT attenuation map scaled to 140 keV, and the third, called "Tl-201", corresponded to the CT attenuation map scaled to 70 keV. Forty replicate noisy sinograms were computed for each data type.

All attenuated projection sets were reconstructed (128x128 grid, pixel size 4 mm) with the conjugate gradient algorithm to solve the penalized frequency weighted least square [PFWLS] criterion defined by (3) and the penalized least square [PLS] criterion defined by (6). All non attenuated data sets were reconstructed with the OSEM algorithm. For all algorithms, the regularization parameter was varied between 2 and 6 pixels when expressed as FWHMs, corresponding to α values ranging from 0.36 to 3.25. Convergence of the reconstruction algorithms was monitored by computing the root mean square error (RMSE) between the images obtained at each iteration and the reference image. Diffusion regularization was compared to the direct filtering of the reference image with the diffusion scheme derived from (4) that is described in [2] using the same values for α. Resolution was assessed by comparing the average of the replicate reconstructions which were virtually noise free. For OSEM, robustness with respect to the amount of noise was also tested by simulating a high noise level corresponding to an acquisition of ten times less counts.

Class-dependent regularization was applied to the Tc-99m noisy data set only, to demonstrate class-dependent noise reduction. The CT attenuation map was segmented into 3 classes: bone and soft tissues (i.e. including blood pool and myocardium), lungs, and background (outside of the body). Four FWHM values were used: 2 pixels for the soft tissues, 4 pixels for the lungs, 6 pixels for the background, and 4 pixels between classes. Selective noise reduction was assessed by considering the difference between the reconstructed image and the images reconstructed with PFWLS and uniform regularization with FWHM values of 2, 4 and 6 pixels.

IV. Results

Convergence of the PFWLS algorithm was monitored when reconstructing noise free Tc-99m data and Tl-201 data with α set to 0.81. With a normalized $T = R_a\Gamma$ in (3b), the spectrum of eigenvalues was kept uniform enough from one attenuation map to the other to maintain the same regularization bias in either case (0.197 for the Tc-99m data and 0.198 for the Tl-201 data). This was not true when monitoring convergence without normalization ($T = R_a$ in (3b), with α set to 0.05). In that case, the matrix describing the highest attenuation had the smallest norm yielding the highest bias and smoothing (bias of 0.225 for the Tc-99m data versus 0.268 for the Tl-201 data).

Figure 2 shows profiles through the heart of the average of the replicate reconstructions for the OSEM algorithm. The regularization FWHM values were 2 (triangles), 4 (circles) and 6 (squares) pixels. The profiles can be compared to the reference image filtered with the diffusion scheme and the same FWHM values (lines). The agreement between the regularization and the diffusion filter is shown by a good superposition of the symbols over the corresponding lines. However, for an FWHM value of 6 pixels, the smallest peak was less smoothed by OSEM than by the diffusion filter. The results obtained from averaging replicate reconstruction with 10 times more noise were identical (profile not shown).

Figure 3 shows profiles at the same level as fig. 2 for the PWLS algorithm. A very good agreement is obtained for a 2-pixel regularization. However, as the regularization level increased, the regularization constraint produced less smoothing than the diffusion scheme.

Figure 4 allows for a direct comparison of the averages of the replicate reconstructions according to the data type, the algorithm and the regularization level. The columns correspond to OSEM, PWLS for Tc99m data, PLS for Tc99m data and PWLS for Tl201 data. Each row shows one level of regularization, from no regularization (0) to a diffusion regularization with an FWHM of 6 pixels. In spite of the variations in the noise level (the noise increased with attenuation), the attenuation maps and the reconstruction algorithms, the regularization output is identical for an FWHM value of 2 pixels. As the FWHM increased, diffusion regularization with PWLS was slightly less smoothed, whereas PLS was noticeably less smoothed. PWLS and PLS results were independent from the attenuation maps.

Figure 5 shows the PFWLS reconstruction of noisy data with a region-dependent regularization of FWHM values of 6 pixels in the background outside of the body, 4 pixels in the lungs, and 2 pixels in all other tissues (left image, inverse grey scale). Images A, B, C are the difference images between the region-dependent regularization and the PFWLS reconstructions with uniform regularization of FWHM value of 2 (image A), 4 (image B) and 6 (image C) pixels. Image A (resp: B and C) shows that the region-dependent regularization had the same smoothing effect over the tissues (resp: lungs and background) than a uniform 2-pixel (resp. 4-pixel and 6-pixel) regularization, as expected. Therefore the PFWLS algorithm regularized with the modified Laplacian operator permitted a modulated noise reduction according to *a priori* defined regions.

V. DISCUSSION

Iterative reconstruction algorithms are used to correct for non-uniform attenuation in SPECT or improve the noise properties of low-count PET data. In order to control the noise increase inherent to tomographic reconstruction of noisy data, regularization is applied. However, setting the proper regularization parameter has proved difficult in clinical routine, due to the fact that a given regularization weight produce different smoothing levels according to the patient dependent model [4]. In the present work, we have proposed three reconstruction criteria whose regularization output was not dependent upon the patient attenuation map or data weighting for reasonable amounts of regularization. For the OSEM and two penalized least squares algorithms, that all produce regularized images based on patient dependent models, it was possible to interpret the regularization constraint as a diffusion scheme, therefore independent from the attenuation map or variance estimates, and to relate the regularization parameter to the parameter of a diffusion scheme taken as an FWHM. For a smoothing level of 2 pixels, the proposed regularization produced the same smoothing effect as the diffusion scheme independently of the attenuation map, the noise level, and the statistical criterion. Since a 2-pixel diffusion filtering is very close to using the Hamming filter with cut-off frequency 0.5 of standard filtered back-projection, this regularization value could be used in all cases, whereas further filtering could be applied after reconstruction with (faster) digital filters. Indeed, higher FWHM values showed less-than-expected filtering, suggesting an increasing interference between attenuation correction and regularization with the PFWLS and PLS algorithms. Why did this interference affect PLS more than PWLS will require further investigation.

Region-dependent diffusion regularization based on anatomical information was also demonstrated in the framework of least square reconstruction. In such a case, high regularization values were used in background areas where precise prediction of the filtering effect was not as important, allowing for the "cleaning" of the image.

VI. CONCLUSION

We have proposed two regularization penalties adapted to the least square, weighted least square and OSEM algorithms that provide the same filtering effect as a diffusion scheme used for Gaussian filtering. Diffusion regularization was independent from the patient model and the regularization parameter was mathematically linked to the FWHM of a Gaussian filter.

VII. REFERENCES

[1] Riddell C, Buvat I, Savi I, Gilardi MC, Fazio F, 2002 Iterative reconstruction of SPECT data with adaptive regularization. *IEEE Trans. Nucl. Science* **49** 2350 -2354

[2] Weickert J, ter Haar Romeny BM and Viergever MA, 1998 Efficient and reliable schemes for nonlinear diffusion filtering *IEEE Trans. Image Processing.* **7** 398-410

[3] Clinthorne NH, Pan TS, Chiao PC, Rogers L and Stamos JA, 1993 Pre-conditioning methods for improved convergence rate in iterative reconstruction *IEEE Trans. Med. Imaging.***12** 78-83

[4] Fessler JA and Rogers WL 1996 Spatial resolution properties of penalized-likelihood image reconstruction: space-invariant tomographs *IEEE Trans. Image Processing.* **5** 1346-1358

[5] Hudson HM and Larkin RS, 1994 "Accelerated image reconstruction using ordered subsets of projection data," *IEEE Trans. Med. Imaging*, **13** 601-609

[6] Zubal IG, Harrell CR and Smith E, 1994 Computerized 3D segmented human anatomy *Med. Phys.* **21** 299-302

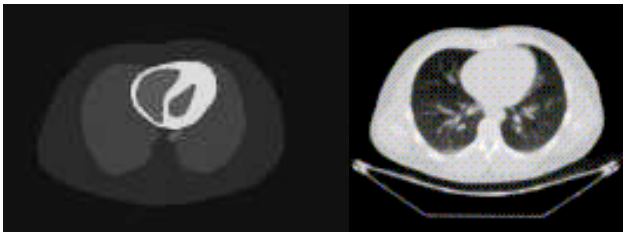

Fig. 1: simulated cardiac emission distribution (left) and CT attenuation map from the Zubal phantom (right).

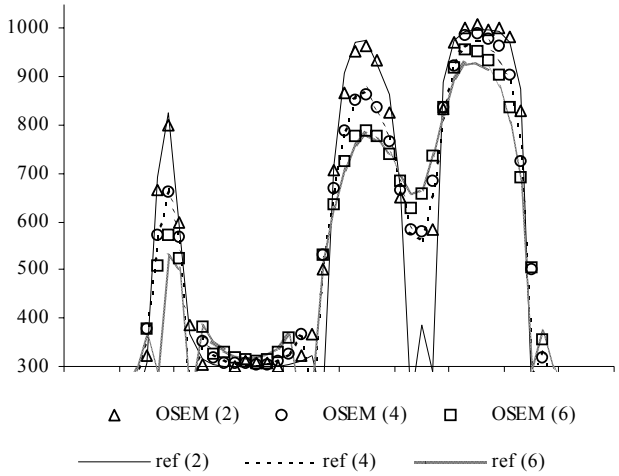

Fig 2: Horizontal profiles through OSEM average reconstruction with FWHM values of 2 (triangles), 4 (circles) and 6 (squares) compared to the reference image filtered with the same FWHM values of 2 (solid line), 4 (dashed line) and 6 (dotted line) pixels.

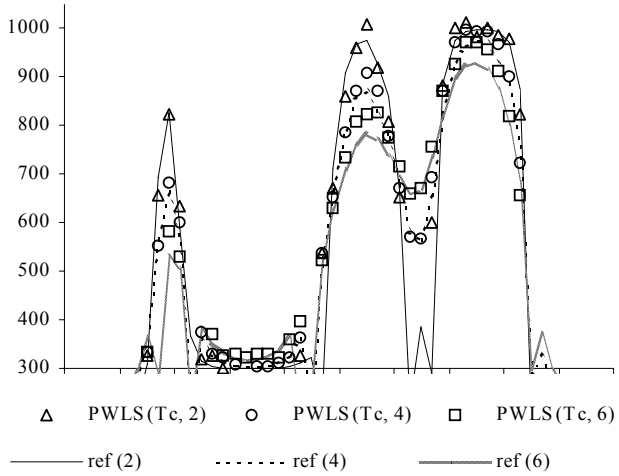

Fig 3: Horizontal profiles through PFWLS average reconstruction with FWHM values of 2 (triangles), 4 (circles) and 6 (squares) compared to the reference image filtered with the same FWHM values of 2 (solid line), 4 (dashed line) and 6 (dotted line) pixels.

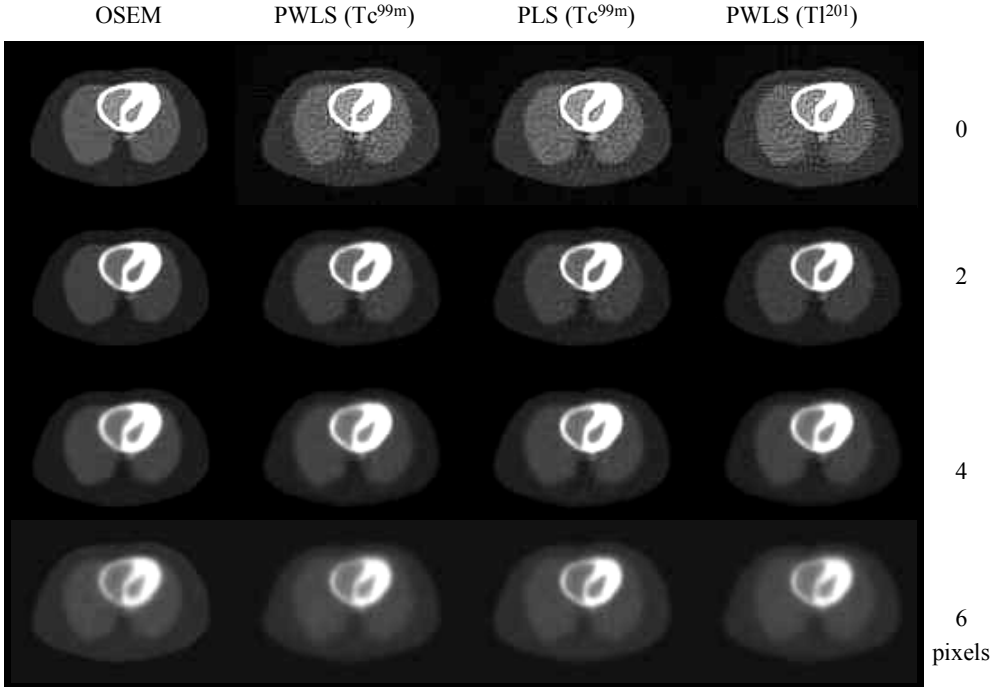

Fig. 4: Average reconstruction for OSEM (1st column), PWLS (2nd column for Tc99m data and 4th column for Tl201 data) and PLS (3rd column) according to the level of regularization (FWHM values from 0 to 6 pixels).

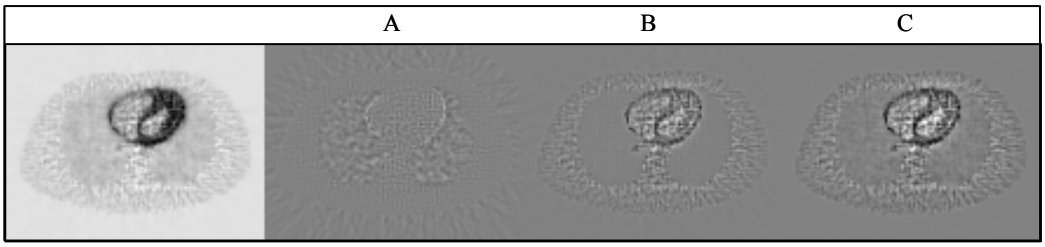

Fig. 5: Left image: PFWLS reconstruction of noisy data with a region-dependent regularization with FWHMs of 6 pixels outside of the body, 4 pixels in the lungs and 2 pixels in all other tissues. Images A, B, C: difference images with PFWLS reconstructions with uniform regularization and FWHM of 2 (A), 4 (B) and 6 (C) pixels.